JOURNAL OF APPLIED ELECTROCHEMISTRY 14 (1984) 269–275

A parametric study of copper deposition in a fluidized bed electrode

M. FLEISCHMANN

Department of Chemistry, University of Southampton, Southampton, SO9 5NH, UK

G. H. KELSALL

Department of Mineral Resources Engineering, Imperial College, London, SW7 2BP, UK

Received 4 February 1983

The behaviour of a fluidized bed electrode of copper particles in an electrolyte of deoxygenated 5×10^{-1} mol dm^{-3} Na_2SO_4–10^{-3} mol dm^{-3} H_2SO_4 containing low levels of Cu(II), is described as a function of applied potential, bed depth, flow rate, particle size range, Cu(II) concentration and temperature. The observed (cross sectional) current densities were more than two orders of magnitude greater than in the absence of the bed, and current efficiencies for copper deposition were typically 99%.

No wholly mass transport limited currents were obtained, due to the range of overpotentials within the bed. The dependence of the cell current on the experimental variables (excluding temperature) was determined by regression analysis. The values of exponents for some of the variables are close to those expected, while others (for concentration and flow rate) reveal interactions between the experimental parameters. Nevertheless the values of the correlation coefficient matrix are low (except for the term relating expansion and flow rate), so that cross terms may be neglected in modelling the system at the first level of approximation.

Nomenclature

- d mean particle diameter (mm)
- E electrode potential, $(\phi_m - \phi_s)_r + \eta(x)$ (V vs ref) where r denotes the value of $(\phi_m - \phi_s)$ at the reversible potential
- I (membrane) current density (A m^{-2})
- L static bed depth (mm)
- M concentration of electroactive species (mol dm^{-3})
- T catholyte temperature (K)
- u catholyte flow rate (mm s^{-1})
- x distance in the bed from the feeder electrode at $x = 0$
- XL expanded bed depth (mm)
- ϵ bed expansion (fraction of static bed depth)
- ϕ_m metal phase potential (V)
- ϕ_s solution phase potential (V)
- ρ_m metal phase resistivity (ohm m)
- ρ_s solution phase effective resistivity (ohm m)
- η 'overpotential' (V)

1. Introduction

Since the first demonstration of the application of the (monopolar) fluidized bed electrode (FBE) [1, 2], this electrode system has been the object of considerable academic [3] and some industrial [4, 5] interest. As with several other recent advances in electrochemical engineering, the FBE resulted from the adaptation of a well established device in chemical engineering to mass transport and scale-up problems in electrochemical reactors. While the physics of its operation at the microscopic level are still a matter of some contention [6–12], there is agreement that its macroscopic performance may typically yield (cross-sectional) limiting current densities more than two orders of magnitude greater than at a planar electrode operating under comparable electrolyte flow rates [13, 14]. This reflects the benefits of a high

0021–891X/84 $03.00 + .12

specific area and high rates of mass transport to the particle surfaces within the bed.

The main advantage of the FBE over its fixed bed counterpart, that during electrodeposition the bed particles grow as discrete entities, has encouraged its use for electrowinning and for treatment of metal-bearing industrial effluents. Correlations exist in the literature [15, 16] to describe the FBE's operation under pure mass transport control, but as in the work reported here, this condition is often inaccessible, due to the range of overpotentials spatially distributed within the bed.

Monhemius and Costa [17] have carried out a 2-level factorial experiment with a fluidized bed electrowinning cell, but such an approach can establish only linear relationships between experimental parameters and the chosen dependent variable(s), current efficiency and 'power consumption'. In view of the usual nonlinear behaviour of electrochemical systems, these 'screening' experiments can be regarded only as a preliminary to a more sophisticated experimental design.

Following Tennakoon's work [13, 18], the investigation described here was an attempt at a more complete empirical description of the macroscopic behaviour of a FBE, operating under less acidic conditions, more typical of industrial effluents than of the 'electrowinning electrolytes' used previously.

2. Experimental details

Fig. 1 illustrates the cell configuration used for all the experiments reported in this paper. A conical diffuser section was used to produce uniform flow and a porous polyethylene disc (Porvair Ltd) ensured uniform fluidization. Contact with the fluidized bed electrode was made with a copper gauze (between 40 and 120 mesh). Solid copper powder (Powder Metallurgy Ltd) sieved into the size ranges of 355–420, 500–420, 500–600, 710–850 and 850–1000 μm, was used as the electrode material. Particles were cleaned in sulphuric acid and washed with deionized water. $Hg/Hg_2SO_4/0.5$ mol dm^{-3} H_2SO_4 reference electrodes could be positioned either just below or above the fluidized bed electrode. All potentials are quoted with respect to this reference with the probe at the top of an expanded bed unless otherwise stated. However, in the regression analysis the appropriate 'overpotential' was used (which included the potential due to ohmic losses in the solution and discontinuous metal phases).

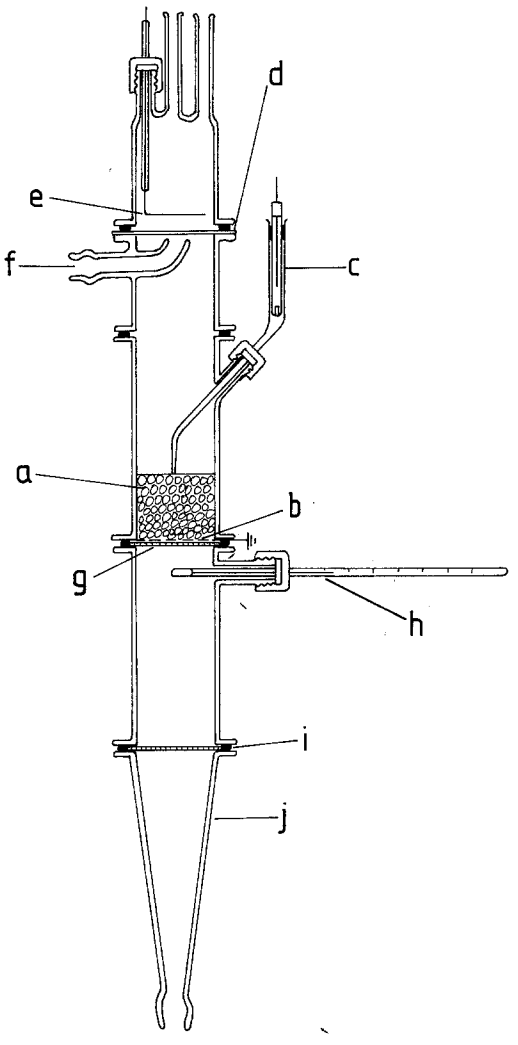

Fig. 1. Fluidized bed electrode cell. a is the fluidized bed of copper particles, b is the copper gauze feeder electrode, c is the reference electrode, d is the ion-exchange membrane, e is the platinum anode, f is the catholyte outlet, g is the porous polythene distributor, h is the thermometer, i is the 'O' ring seal and j is the diffuser.

An ion exchange membrane (Permaplex C–20) was used to separate the catholyte and anolyte so as to prevent oxygen liberated at the flat spiral platinum anode from mixing with the catholyte stream. The supporting electrolyte, 5×10^{-1} mol dm^{-3} Na_2SO_4 + 10^{-3} mol dm^{-3} H_2SO_4 was contained in a 50 dm^3 polythene drum fitted with a nitrogen bubbler to deoxygenate the solution;

slightly acid conditions were necessary to prevent the formation of surface oxide on the electrode particles. The remaining parts of the flow circuit consisted of a polypropylene pump (Totton Electrical Ltd, Type PCP 175 with ceramic shaft and magnetic coupling) together with 'Rotameter' flow meters (GEC-Elliott Ltd) fitted with 'Korannite' ceramic floats and polythene tubing adaptors; an angle seat valve (G. Fischer Ltd) controlled the flow rate. The only metallic materials in the whole circuit were therefore the fluidized bed electrode and the gauze 'feeder' electrode.

Experiments were carried out at controlled potential, a potential linear sweep generator being used for measurements of polarization curves. Current efficiencies were determined by using a current integrator together with measurements of concentration changes by means of atomic absorption spectrophotometry. Under the conditions used in the experiments reported here current efficiencies were typically greater than 99%.

Pre-electrolyses of the base electrolyte were carried out (mainly to remove residual oxygen) until the cell current at the working potential was $\leqslant 1$ mA. A calculated quantity of a concentrated copper sulphate solution was then introduced into the catholyte using a hypodermic syringe via a serum cap, the solution being mixed thoroughly at high flow rate before the cell was switched into the circuit.

3. Results

Fig. 2a shows that diffusion limited current plateaux could not be observed under the conditions used here, in contrast to the results of Tennakoon [13, 18]. This is due to the lower solution conductivity of the supporting electrolyte (5×10^{-1} mol dm^{-3} Na_2SO_4 + 10^{-3} mol dm^{-3} H_2SO_4 in contrast to 1 mol dm^{-3} H_2SO_4). In view of the relatively high solution resistivity, part of the fluidized bed electrode was always under activation control (region of E_{min}) rather than under diffusion control, provided the applied overpotential, η_{max}, was maintained below the value for the onset of hydrogen evolution, Figs. 3a and b. This mixed activation–diffusion control is also responsible for the relatively linear polarization plots. Equally, mixed control is indicated by the value of the observed activation energy (≈ 33 kJ mol^{-1}),

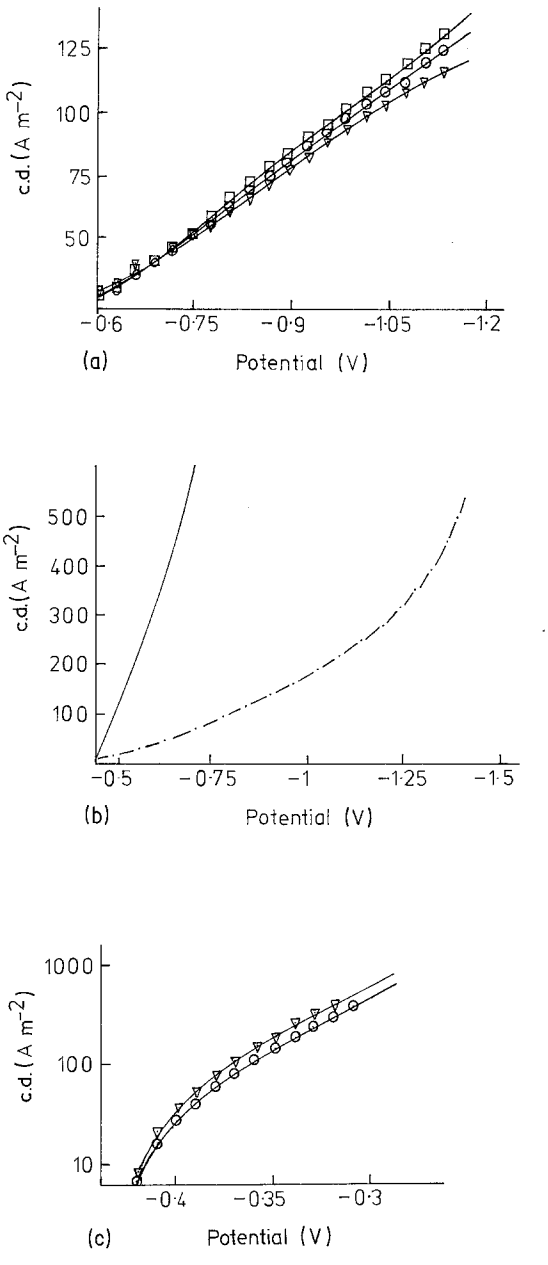

Fig. 2. (a) Effect of flow rate on the cathodic polarization behaviour of the FBE. 5×10^{-1} mol dm^{-3} Na_2SO_4 – 10^{-3} mol dm^{-3} H_2SO_4 – 2×10^{-4} mol dm^{-3} $CuSO_4$ electrolyte. 100 g 710–850 μm Cu particles, $L = 13$ mm. ▫ $u = 53$ mm s^{-1}, $XL = 20.5$ mm; ○ $u = 41$ mm s^{-1}, $XL = 18.5$ mm; ▽ $u = 29$ mm s^{-1}, $XL = 16.5$ mm. (b) Influence of the position of the reference electrode probe on the cathodic polarization behaviour. Reference electrode probe: —— below bed, –·– on top of expanded bed. 5×10^{-1} mol dm^{-3} Na_2SO_4 – 10^{-3} mol dm^{-3} H_2SO_4 – 1.5 ppm $CuSO_4$ electrolyte. 200 g 710–850 μm Cu particles, $L = 29$ mm, $u = 40$ mm s^{-1}, $XL = 34$ mm. (c) Effect of flow rate on the anodic polarization behaviour. Same conditions as in (a).

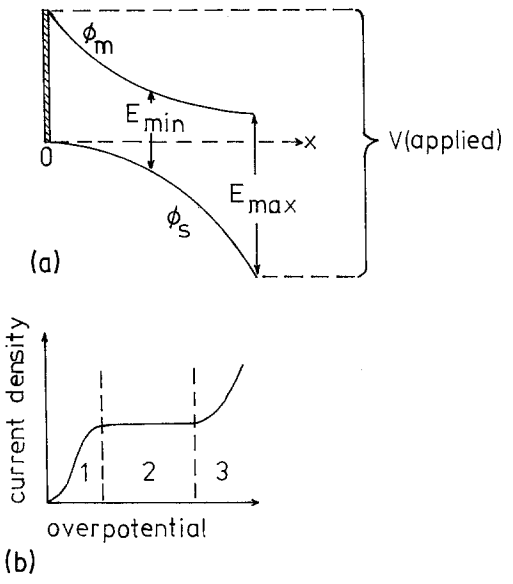

Fig. 3. (a) Schematic potential profiles as a function of the distance x from the feeder electrode ($x = 0$) for the metal phase (ϕ_m) and solution phase (ϕ_s). The electrode potential $E = (\phi_m - \phi_s)_r + \eta(x)$, E_{min} being the minimum value in the middle of the bed, $\eta(x) = \eta_{min}$, and E_{max} the maximum value at the top of the bed, $\eta(x) = \eta_{max}$. V (applied) is the potential applied between the reference electrode probe at the top of the expanded bed, and the feeder electrode at the bottom. (b) Schematic polarization curve for copper deposition. Region 1: mainly activation control, region 2: diffusion control, region 3: hydrogen evolution in parallel with diffusion controlled copper deposition.

as derived from the data in Fig. 4d. This value lies between those expected for activation and pure diffusion control.

Fig. 2b shows the effect of changing the position of the reference electrode which is readily interpreted in terms of Fig. 3a: the overpotential at the top of the bed will exceed the potential applied to the feeder electrode below the bed in this case. In contrast to the cathodic polarization curves, the anodic plots show a relatively simple behaviour, Fig. 2c. The whole electrode will now be under activation control, and at high potentials the curves approach a Tafel line having a slope twice that predicted for the well-known reaction scheme [19]

$$Cu \xrightarrow{\text{slow}} Cu^+ + e \qquad (1)$$

$$Cu^+ \rightleftharpoons Cu^{2+} + e \qquad (2)$$

This doubling of the Tafel slope, due to the distribution of the potential within the electrode, Fig. 3a, is observed for packed and fluidized bed electrodes of sufficient length [20, 21].

The lack of a diffusion controlled limiting current plateau for the cathodic reaction precludes a simple analysis in terms of mass transfer coefficients and dimensionless groups [15, 16, 22]. The conditions used here are probably typical of a range of possible application of fluidized bed electrodes and it is evident that many parameters determine the behaviour of the system *inter alia* the molarity, M (mol dm^{-3}), overpotential, η (V), the solution and metal phase resistivities, ρ_s and ρ_m respectively (ohm m), the mean particle diameter, d (mm), static bed depth, L (mm), catholyte flow rate, u (mm s^{-1}), bed expansion, ϵ (fraction of packed bed depth) and catholyte temperature, T(K). The normal experimental approach when so many parameters are involved has been to vary one parameter at a time while monitoring the response of the dependent variable (here it is the current density I, A m^{-2}) and attempting to keep all other variables constant. This method risks oversimplification if not misrepresenting the system's behaviour as it does not take into account any interactions between the various parameters, i.e. the 'partial regression coefficients' only are determined.

A considerable data base was therefore collected and treated by regression analysis [23] as described elsewhere [24]. Figs. 4a–e illustrate some of these measurements. The concentration dependence, Fig. 4a, is seen to be markedly nonlinear and this nonlinearity must be due to the decrease in the relative proportions of the bed under mass transfer as compared to kinetic control, Figs. 3a and b, due to changes in the potential distribution with increase of concentration.

The complex effects of changes of current with flow rate for the various particle size ranges, Fig. 4b, show the trade-off between enhanced rates of mass transfer with increasing flow rate and the increased bed expansion which causes an increase in the potential drop in the metal phase, Fig. 3a, due to the increase of the resistivity [6, 9, 12]. At low flow rates mass transport is rate limiting while at high flow rates (depending on the particle size) charge transfer within the discontinuous metal phase limits the cell current.

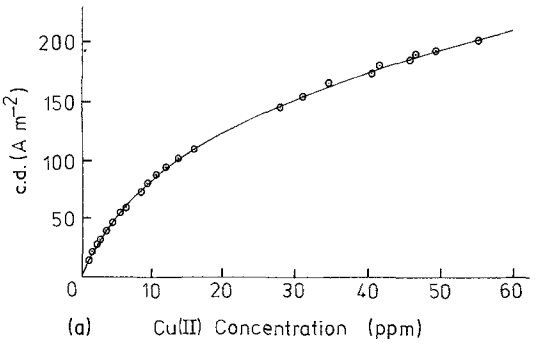

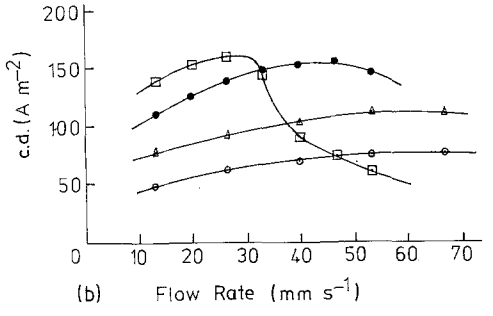

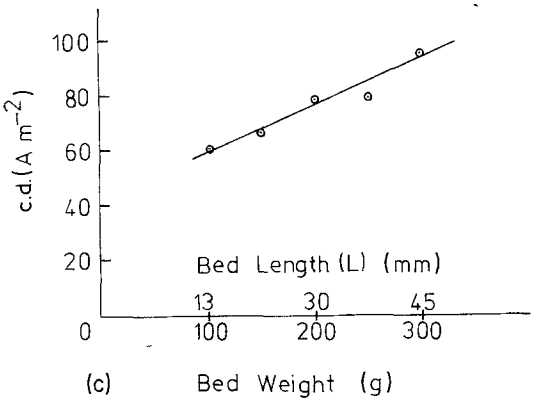

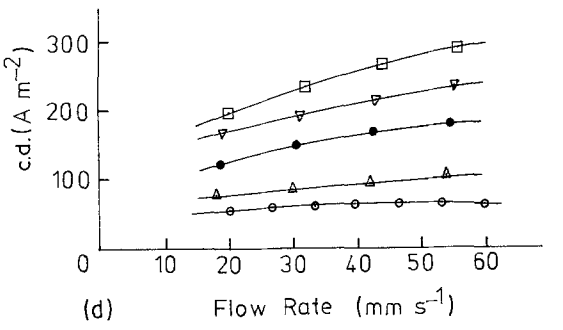

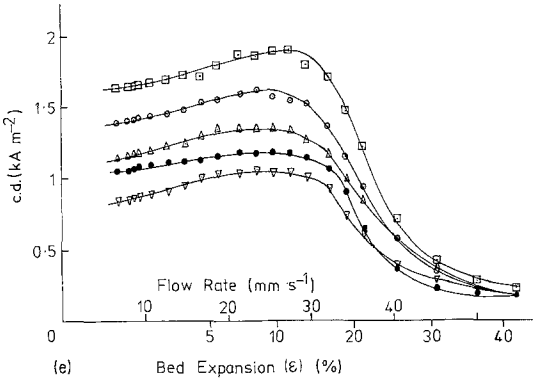

Fig. 4. (a) Effect of Cu(II) concentration on FBE current density. 5×10^{-1} mol dm^{-3} Na_2SO_4 – 10^{-3} mol dm^{-3} H_2SO_4 – x ppm $CuSO_4$ electrolyte. 100 g 710–850 μm Cu particles, $L = 13$ mm, $u = 53$ mm s^{-1}, $XL = 18.5$ mm, $T = 293$ K, – 1.0 V applied. (b) Effect of particle size range and flow rate on FBE current density. 5×10^{-1} mol dm^{-3} Na_2SO_4 – 10^{-3} mol dm^{-3} H_2SO_4 – 10^{-4} mol dm^{-3} $CuSO_4$ electrolyte, $T = 293$ K. 100 g Cu particles: ▫ 355–420 μm, • 500–600 μm, △ 710–850 μm, ⊙ 850–1000 μm, – 1.0 V applied. (c) Effect of bed length on FBE current density. Electrolyte as in (b) $u = 41$ mm s^{-1}, – 1.0 V applied. (d) Effect of temperature/flow rate on FBE current density. Electrolyte as in (b). 100 g 710–850 μm Cu particles: ⊙ 293 K, △ 303 K, • 313 K, ▽ 323 K, ▫ 333 K. (e) Effect of Cu(II) concentration/flow rate/bed expansion on FBE current density. 5×10^{-1} mol dm^{-3} H_2SO_4 – x ppm $CuSO_4$ electrolyte 200 g 500–600 μm Cu particles, $L = 30$ mm, $T = 298$ K, – 0.96 V applied. ▫ 470, ⊙ 376, △ 248, • 167, ▽ 126 ppm Cu(II).

The effect of bed height, Fig. 4c, is approximately linear. The fact that the line has a low gradient and does not pass through the origin can again be attributed to the profiles, Fig. 3a, since the most active zones are confined to the top and bottom of the bed. Enhanced mass transfer at the bottom of the bed due to hydrodynamic entry effects [7] must also contribute to the displacement of the line from the origin.

The effect of temperature on the current vs flow rate relationship is shown in Fig. 4d. The current densities at 303 K were abnormally low as this sequence of measurements was taken immediately after pre-electrolysis of the solution. The pre-electrolysis produced a smooth bright surface on the bed particles due to a mechanically assisted cathodic smoothing process (the force in the particle impacts is of the order of the yield stress for a

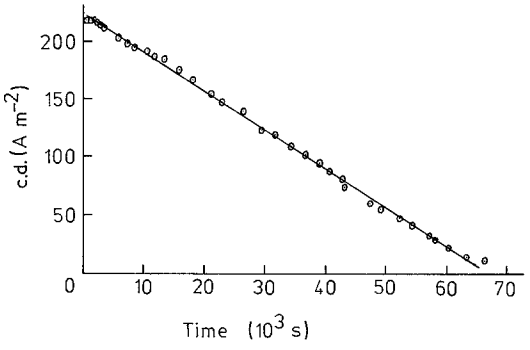

Fig. 5. Current density vs time relationship for the recycle electrolysis of 50 dm^3. 5 × 10^{-1} mol dm^{-3} Na_2SO_4 – 10^{-3} mol dm^{-3} H_2SO_4 – 10^{-3} mol dm^{-3} $CuSO_4$. 100 g 710–850 μm Cu particles, L = 13 mm, XL = 18.5 mm, u = 53 mm s^{-1}. – 1.0 V applied.

metal such as copper [6]). Deposition following such cathodic smoothing inevitably led to a roughening of the surface over a limited time period (see below).

It would be difficult to describe the temperature effect theoretically since so many parameters are affected: ρ_m and ρ_s and consequently the distribution of potential in the bed, the kinematic viscosity and its effect on the hydrodynamics, the diffusion coefficient of the copper ions and the electrode kinetics. The marked increase of current density with temperature, however, suggests that the last factor plays a major role and that at least part of the electrode was under activation control.

In order to illustrate the effect of ρ_s on the performance of the electrodes, some current density vs flow rate data obtained in 0.5 mol dm^{-3} H_2SO_4 are shown in Fig. 4e. Although the copper ion concentrations are somewhat greater than those used in the other series of experiments, the current densities are considerably higher than those expected from an extrapolation of results using 0.5 mol dm^{-3} Na_2SO_4 + 10^{-3} mol dm^{-3} H_2SO_4.

Finally, Fig. 5 shows the depletion of 10^{-3} mol dm^{-3} $CuSO_4$ (63.5 ppm) from the 50 dm^3 tank. Clearly the current–time curve is far from an exponentially decaying function expected for such a coulometric experiment [2, 3] although a current efficiency of 99% was achieved, in agreement with earlier results [12]. This deviation of the observed from the expected shape is again due to the complex changes of the distribution of potential within the bed, in this case caused by the decreasing concentration with increasing time. Clearly the proportion of the bed under diffusion control (see Fig. 3b) will increase with time, so that the current will decay less slowly than would be expected for a uniformly active bed. A secondary feature observed is the region of constant current at short times notwithstanding a decrease in the copper ion concentration: this is due to a progressive roughening of the initially smooth surface of the particles produced during pre-electrolysis (see above). This effect is more marked in more dilute solutions where an increase of current with increasing time can be observed.

4. Discussion

It was found that the data obtained in this investigation could be fitted by the equation

$$I = 2126 d^{-1.11} L^{-0.09} \eta^{1.17} \epsilon^{-0.08} M^{0.40} u^{0.20} \quad (3)$$

for the range of conditions specified in Fig. 4. In the fitting procedure the variable T had to be excluded as the data base was insufficient to allow an adequate specification of the cross correlation coefficients with respect to this variable. For the restricted analysis represented by this equation the 90% confidence limits showed that the exponents were well estimated except that the coefficients for L lay in the range – 0.122 to 0.054 and ϵ in the range – 0.1 to – 0.056. It is significant that these two parameters were those containing the largest errors, as the bed lengths were merely read from a graduated scale. Nevertheless, the negative exponent of L is surprising bearing in mind the data in Fig. 4c: it is probably due to the inclusion of data for which the current densities were anomalously low (probably due to the surface smoothing effect).

The exponents for d and η are much as expected from Figs. 4b and 2a, tending to confirm the previous explanations of such dependence. However, those for M and possibly u are a little lower than expected from Figs. 4a and b. A logarithmic plot of the data in Fig. 4a shows a current density dependence of $M^{0.5}$ increasing to $M^{0.7}$ at low M. The lower value obtained by the regression analysis is due to the allowance for interaction with other parameters.

The overall standard error of residuals (i.e.

observed–calculated current density) was 1.32 $A\,m^{-2}$, which showed a reasonably good fit of the desired equation with the experimental results. The correlation coefficient matrix showed the expected high [0.86] correlation between expansion and flow rate. Other values were $\leqslant 0.5$ and typically in the range 0.1–0.2. This general analysis of the operation of the fluidized bed electrode (which we emphasize is a generally valid procedure) therefore shows that the cross terms can in fact be neglected in modelling at the first level of approximation. An interpretation of the data in terms of models of the FBE will be published later [26].

References

[1] J. R. Backhurst, M. Fleischmann, F. Goodridge and R. F. Plimley, British Patent 1 194 181 (1970).

[2] J. R. Backhurst, J. M. Coulson, F. Goodridge, R. E. Plimley and M. Fleischmann, *J. Electrochem. Soc.* **116** (1969) 1600.

[3] F. Coeuret, *J. Appl. Electrochem.* **10** (1980) 687.

[4] J. A. E. Wilkinson and K. P. Haines, *Trans. Inst. Min. Metall.* **81** (1972) C157.

[5] G.Van der Heiden, C. M. S. Raats and H. F. Boon, *Chem. Ind.* **13** (1970) 465.

[6] M. Fleischman and J. W. Oldfield, *J. Electroanal. Chem.* **29** (1971) 231.

[7] F. Goodridge, D. I. Holden, H. D. Murry and R. F. Plimley, *Trans. Inst. Chem. Eng.* **49** (1971) 128.

[8] *Idem, ibid.* **49** (1971) 137.

[9] G. Kreysa, *Electrochim. Acta* **25** (1980) 813.

[10] J. W. Evans and B. J. Sabacky, *AIChE Symp. Ser.* **74** (1978) 145.

[11] *Idem. Metall. Trans.* **8B** (1977) 5.

[12] A. A. C. M. Beenackers, W. P. M. van Swaaij and A. Welmers, *Electrochim. Acta* **22** (1977) 1277.

[13] M. Fleischmann, J. W. Oldfield and L. Tennakoon, *J. Appl. Electrochem.* **1** (1971) 103.

[14] D. Drazic, R. Atanasoski and S. Zecevic, *Hem. Ind.* **28** (1974) 149.

[15] D. J. Pickett, *J. Appl. Electrochem.* **5** (1975) 101.

[16] A. T. S. Walker and A. A. Wragg, *Electrochim. Acta* **25** (1980) 323.

[17] A. J. Monhemius and P. L. N. Costa, *Hydrometallurgy* **1** (1975) 183.

[18] C. L. K. Tennakoon, PhD thesis, Southampton University (1971).

[19] E. M. Mattson and J. O'M. Bockris, *Trans. Faraday Soc.* **55** (1959) 1586.

[20] J. S. Newman and C. W. Tobias, *J. Electrochem. Soc.* **109** (1962) 1183.

[21] M. Fleischmann and J. W. Oldfield, *J. Electroanal. Chem.* **29** (1971) 211.

[22] M. Fleischmann and I. N. Justinijanovic, *J. Appl. Electrochem.* **10** (1981) 143.

[23] O. L. Davies and P. L. Goldsmith (eds.), 'Statistical Methods in Research and Production', Longman, London (1972).

[24] G. H. Kelsall, PhD thesis, Southampton University (1975).

[25] A. T. S. Walker and A. A. Wragg, *Chem. Eng. Sci.* **35** (1980) 405.

[26] M. Fleischmann and G. H. Kelsall, to be published.